Experience with Out-of-Step Relaying and Lessons Learned on the California-Oregon Intertie

Caitlin Martin, BPA   Aaron Martin, BPA

Western Protective Relay Conference Paper 2020

Abstract-- **Microprocessor based Out-of-Step relays have been used on the California-Oregon Intertie since the 1980's to control separation of the north and south systems early in an otherwise unrecoverable power swing. In 2017, the then 25 year old relays were identified for replacement, which initiated the need for updated transient stability swing studies and relay testing. This paper will go through the relay settings, and testing with both simulated and real measured data. Additional topics of this paper include: determining the voltage source location on a series compensated line, converting transient stability simulation results to relay test input data, and an analysis of the 2019 out-of-step relay misoperations.**

Index Terms— **Out-of-Step, Out-of-Step relay, power swing**

I. Introduction

POWER swings can occur after a disturbance and oscillate at a sub-synchronous frequency. Stable power swings are recoverable without intervention. An unstable swing requires intervention of a Remedial Action Scheme (RAS) or out-of-step (OOS) tripping relaying to prevent or isolate the collapse of a system. OOS tripping protection is the focus of this paper. OOS tripping relays are used to separate systems in a controlled way at a specific location early in an unstable power swing. OOS blocking prevents separation during an unstable power swing in undesirable locations.

The OOS tripping relays, that are the focus of this paper, are located at Malin and Captain Jack substations for the three 500 kV California-Oregon Intertie (COI) lines: Malin-Round Mountain 1 & 2, and the Captain Jack-Olinda. The lines run north and south on the west coast of the United States as shown in Fig. 1.

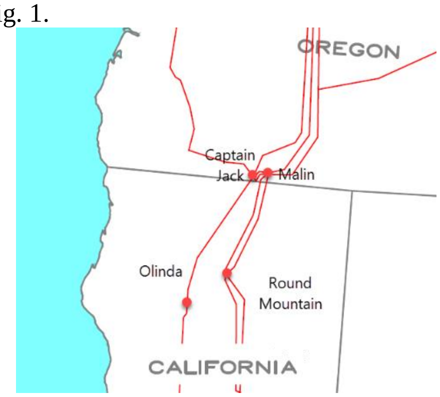

Fig. 1. Geographical location of OOS trip relays at Malin and Captain Jack substations.

Each line is also series compensated with line-end capacitors at each substation as shown in Fig. 2.

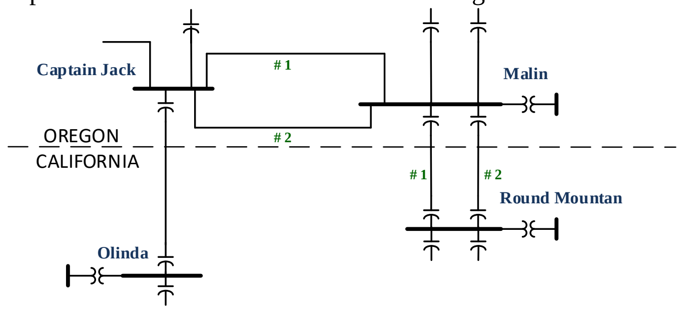

Fig. 2. COI transmission lines with OOS trip relays.

II. Out-of-Step Tripping Relay Settings

OOS tripping relays need to distinguish an unstable power swing from a stable power swing, a fault, and from load flow. Relays can do this in a few different ways. One method is by implementing inner and outer impedance blinders that can be rectangular (quadrilateral), circular (mho), or some combination of the two.

The event is tracked as it comes between the blinders and the resistive speed is measured in ohms-per-second. Faults are fast-changing events, and swings are slow in comparison. The blinders need to be set where the relay can detect an unstable swing from a stable swing or load encroachment.

Stable swings on the COI tend to oscillate in a focused area on an R-X plot, and may reach in between the blinders and back out the way it came in. An unstable swing on the COI tends to create a large slow swinging loop passing through both inner and outer blinders (See Fig. 3). An internal fault will also pass through both blinders, but will be fast moving. Load characteristics are system dependent, and as discovered on the COI can change over time.

Another important factor is that unstable swings on the COI tend to occur under heavy loading. To prevent an unnecessary separation under light loads a supervisory minimum pickup current element is also used.

Caitlin Martin and Aaron Martin are with Bonneville Power Administration. Vancouver. WA 98663 USA.

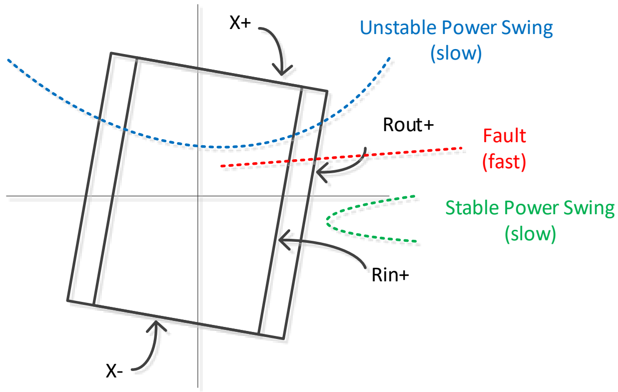

Fig. 3. OOS characteristics on an impedance R-X plot with example power swings and fault.

III. Out-of-Step Relaying History

The first microprocessor OOS relays were installed on the COI in 1982 which operated on resistance magnitude and speed only. Two IEEE papers were written on this topic [1] [2].

In 1992 they were upgraded to a new relay that implemented the OOS quadrilateral characteristic with inner and outer blinders that included resistance and reactance settings, resistance rate of change, and a minimum pickup current. The OOS relays used were early versions of microprocessor line distance relays. They were set to trip for a swing at or below 400 ohms/sec with the resistive inner blinder set to 40 ohms and outer blinder set 50 ohms primary as shown in Fig. 4.

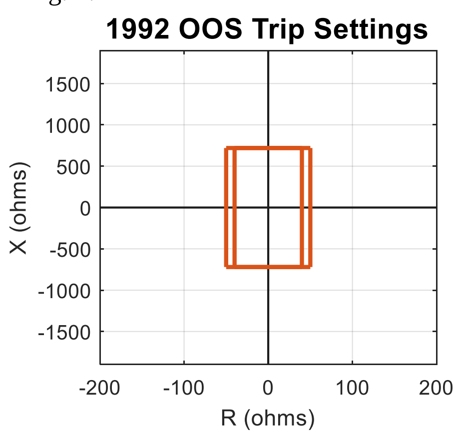

Additional OOS Trip Settings	
Minimum PU Current (A)	600
Maximum Resistive Rate of Change (ohm/sec)	400

Fig. 4. 1992 OOS trip relay characteristic R-X plot and additional settings.

In 2016 and 2017 the solid state line relays on the Malin-Round Mountain lines 1 & 2 were replaced with modern microprocessor relays. Also slated to be replaced were the OOS microprocessor relays that had been installed in 1992 at Malin.

Because the same manufacturer of the OOS microprocessor relays installed in 1992 were being applied for the new line protection relays, design engineers made the decision to move the functionality of the OOS relays into the new line distance relays. Protection engineers then decided to apply the same 1992 OOS settings.

BPA, who is responsible for the Malin end of the lines, coordinated the settings with the engineers from Pacific Gas and Electric (PG&E) who are responsible for the Round Mountain end of the line. PG&E performed transient testing with hardware-in-the-loop equipment to validate the line protection and the OOS settings. The PG&E testing method automates the fault simulation and data collection, allowing them to run thousands of test cases in a short period of time [3]. In one batch of 10,000 tests the OOS trip element picked up for approximately 2.5% of the internal faults. In another batch of 5,000 external faults on adjacent and parallel lines the OOS trip element picked up for approximately 30% of the faults. The performance of the OOS trip settings was unsatisfactory.

Fig. 5 below is an example of an AB phase fault 95% down the Malin-Round Mountain 1 line from the Malin end and is one of the faults that the OOS trip element Misoperated for. The impedance is shown as green dots, the original 1992 OOS trip element that was used during testing is shown in red. Prefault load impedance is outside of the OOS trip element blinders. As the fault develops it enters the blinders as expected, but unexpectedly caused a trip operation. The trip likely was due to the time the fault spent between the blinders was long enough to appear as a slow swing.

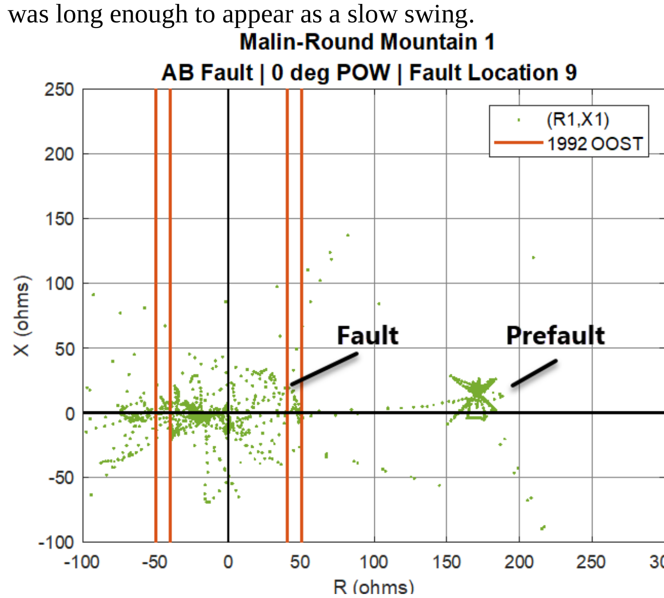

Fig. 5. Impedance plot of simulated internal AB fault overlaid with the 1992 OOS trip characteristic.

The hardware in the loop testing demonstrated that applying the original OOS trip elements to the new line relays with the existing settings was not a feasible option. It was decided at the time to keep the existing OOS trip relays on the line until the scheme could be extensively studied.

At that time, the BPA planning engineering group was consulted and they agreed that BPA still needed OOS trip relays on the three intertie lines, as the OOS trip relays are part of a RAS safety net scheme. BPA's protection engineering group reviewed the original OOS tripping scheme and requested a fresh stability review from the planning engineers.

A senior engineer in the protection group recollected that the OOS trip relays were to be connected to the breaker side of the series capacitors, not on the line side as they were at the time.

In 1996 the local engineer responsible for the relays had moved the voltage connections of the OOS relays to the line side of the capacitors to take advantage of the impedance fault location feature as shown in Fig.6.

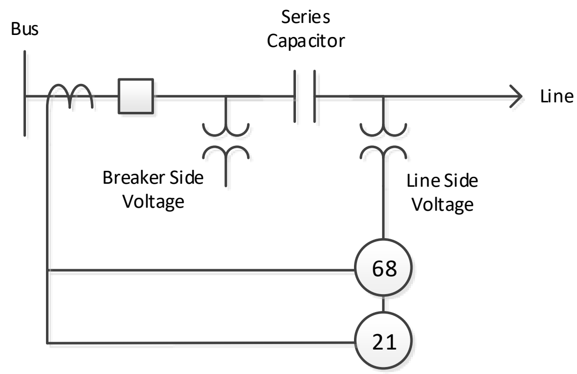

Fig. 6. OOS trip relay (68) and distance relay (21) both on the line-side voltage connection.

The OOS relays voltage inputs were put back on the breaker side of the series capacitors after the discovery was made as shown in Fig.7.

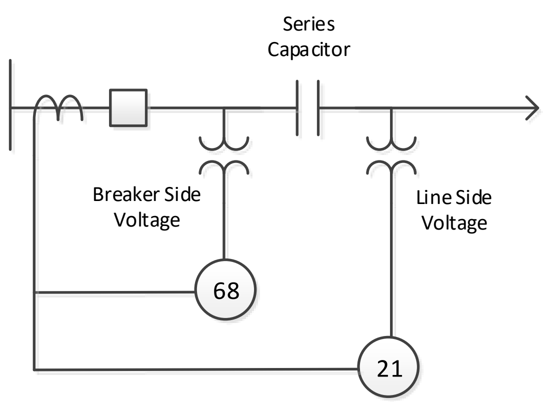

Fig. 7. OOS trip relay (68) using the breaker-side voltage, while the distance relay (21) uses the line-side voltage connection.

Since 1996 until their removals in 2018 and 2019 there were no OOS relay operations for any disturbance including the 1996 west coast outages.

BPA considered the following three options to replace the OOS relays:

1) Use a line relay connected to the line-side PT for both OOS and distance protection.
2) Use a line relay that can support two voltage sources, so that the OOS protection can use the breaker-side PT and line distance protection can use the line-side PT. (Fig. 8)
3) Use a separate OOS relay connected to the breaker side PTs of the series cap. (Fig. 7)

Because the OOS swing cases provided by planning used breaker-side voltages, and the distance relay elements of the new line relays had been successfully tested using the line-side voltage, option 1 was not desirable. For option 2 to work, the line relays required two three-phase voltage inputs, so that the OOS trip element could use the breaker-side voltage and the distance element could use the line-side voltage. Option 3 would only be considered if option 2 and option 1 were not viable. Fortunately, the second set of line relays supported two independent three-phase voltage inputs as shown below in Fig. 8.

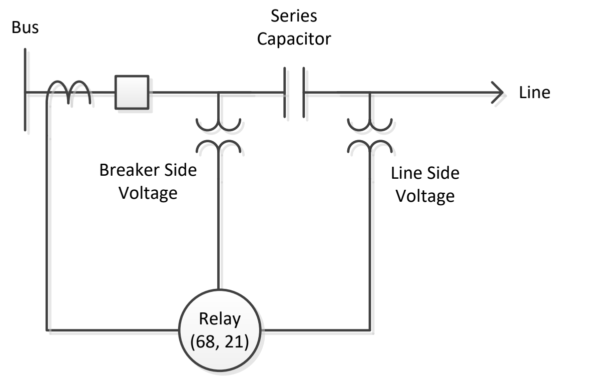

Fig. 8. OOS trip (68) function and distance (21) function in the same relay. The OOS trip function uses the breaker side, while the distance function uses the line-side voltage connection.

IV. Series Capacitor Line Side and Breaker-Side Voltage Differences

For a line-end series-compensated line, the voltage on the line side and the breaker side are going to differ when the capacitors are in-service. Since the breaker-side voltage is more stable, it was selected for use in the OOS relay.

A recent single line-to-ground fault on the Captain Jack-Olinda line illustrates the difference between the breaker side and the line-side voltage of the series capacitor before and during a fault. During the fault, the voltage difference was most notable with a shift in the magnitude and phase angle. (see Fig. 9 and 10). The line-side voltage (red) is leading the breaker-side voltage (green) by about 28 degrees during the fault. The peak voltage difference during the fault is about 9%. This results in a shift of impedance depending on what voltage is used as shown in Fig 11.

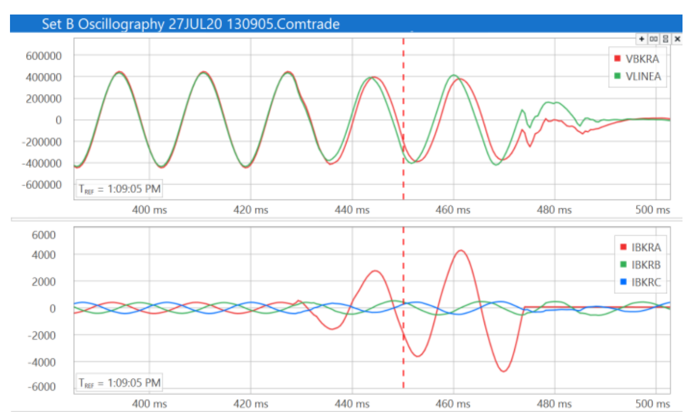

Fig. 9. Captain Jack line relay event record. [top] Faulted phase breaker side (red) and line-side voltages (green), [bottom] three-phase line currents with the faulted phase in red.

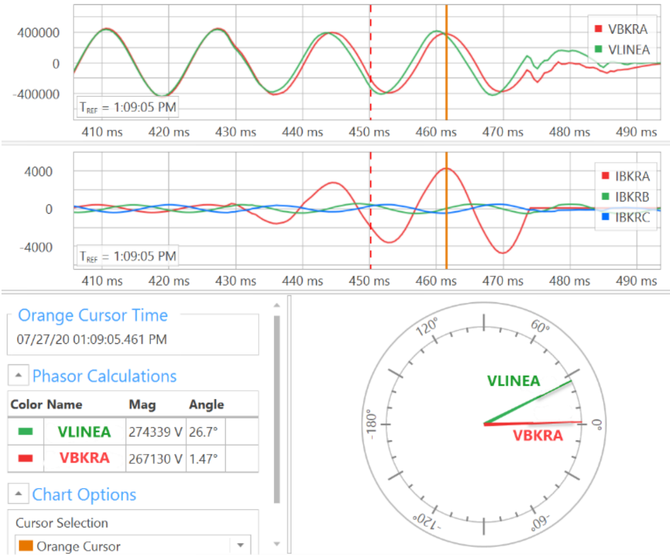

Fig. 10. Same event as previous figure zoomed in at the end of the fault with the phasor diagram plot at the bottom for the time of the horizontal orange cursor.

In Fig.11 the calculated positive sequence impedance using the breaker-side voltage is shown in red and the calculated impedance using the line-side voltage is shown in green. Prefault impedance shows up as a star in the lower right-hand side of the plot, while the fault impedance shows up on the upper left-hand side of the plot. Note that although the general trajectory is the same, there is a notable shift between the two impedances that is variable. The breaker-side voltage which includes the series capacitor is shifted in the negative reactance direction as expected.

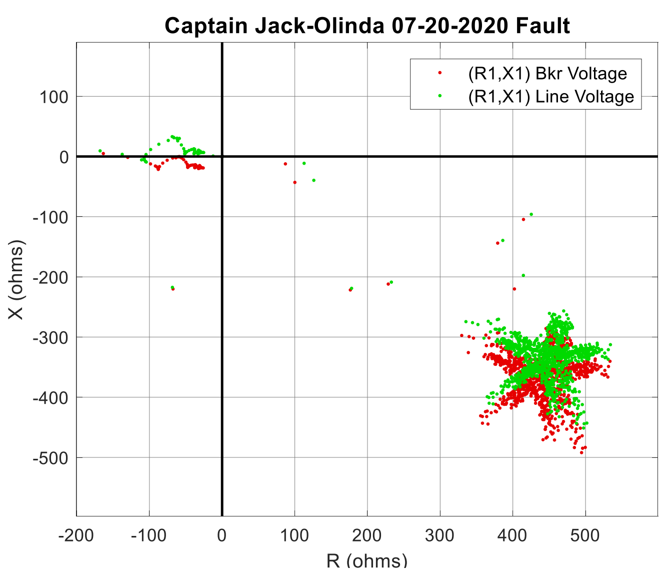

Fig. 11. Same single line-to-ground fault as in Fig. 9 and Fig.10 plotted on an R-X plane using the breaker side (red) or line-side voltage (green).

V. Out-of-Step Relay Testing Process & Lessons Learned

Transmission Planning proposed the following OOS trip relay settings for the Malin-Round Mountain 1 & 2 and Captain Jack-Olinda lines that are also plotted in Fig. 12:

- Maximum rate of change for the swing impedance is 200 ohms per second.
- The inner and outer blinders are 40 and 60 ohms of resistance respectively.

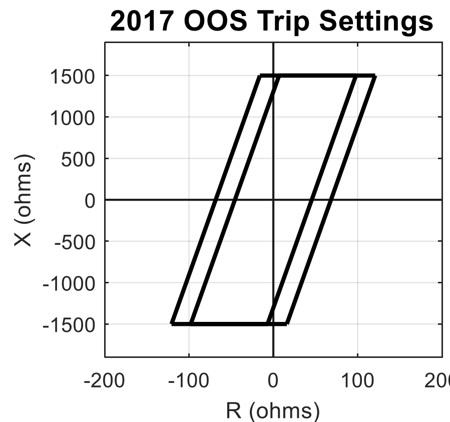

Additional OOS Trip Settings	
Minimum PU Current (A)	300
Maximum Resistive Rate of Change (ohm/sec)	200

Fig. 12. OOS trip impedance characteristic for new relays developed in 2017 and additional settings.

Transmission Planning ran updated transient stability power swing studies to develop the settings and provided comma-separated values (CSV) files in July of 2017 that included both stable and unstable power swings. The CSV files contained RMS power flow measurements that were not directly compatible for relay testing. The data needed to be converted into sinusoidal three-phase peak values in IEEE C37.111 Common format for transient data exchange (COMTRADE) for relay testing. Once converted the COMTRADE files could then be played directly into the relays. The relay event files could be analyzed to ensure proper trip operations for unstable power swings, and no trip operations for stable power swings.

The flowchart illustrated in Fig. 13 outlines this process that took until 2018 to complete. Although, the figure implies a linear progression there were loopbacks where results were not as expected, and the relays needed to be retested. In Fig. 13 the blue documents represent a file created by the previous process.

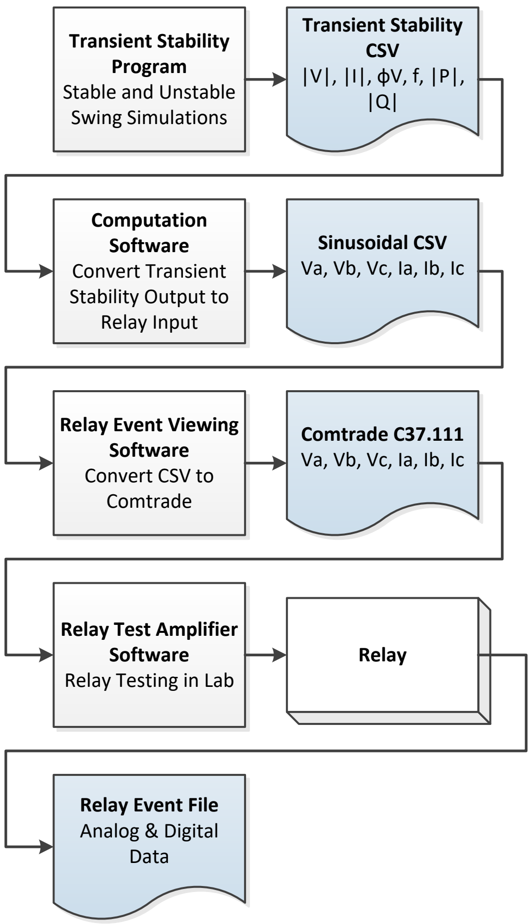

Fig. 13. Process used to test OOS trip relay settings.

A. *Transient Stability Program Swing Simulations*

Transmission Planning provided three stable and three unstable simulated power swings. Fig. 14 and 16 show the RMS time-domain plots of the six events. Fig. 15 and 17 show the impedance plots for each event.

In the three simulated unstable cases shown in Fig. 14 there is an initial swing where the Malin bus voltage dips below 200 kV L-L RMS. It is unlikely that the nominal 525 kV L-L RMS system would continue to swing after this dip as shown in the simulations. However, it is included in the relay testing to verify separation would occur prior to this point.

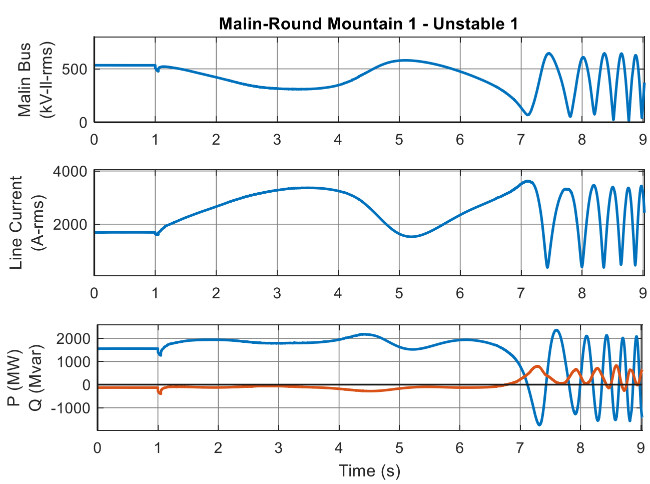

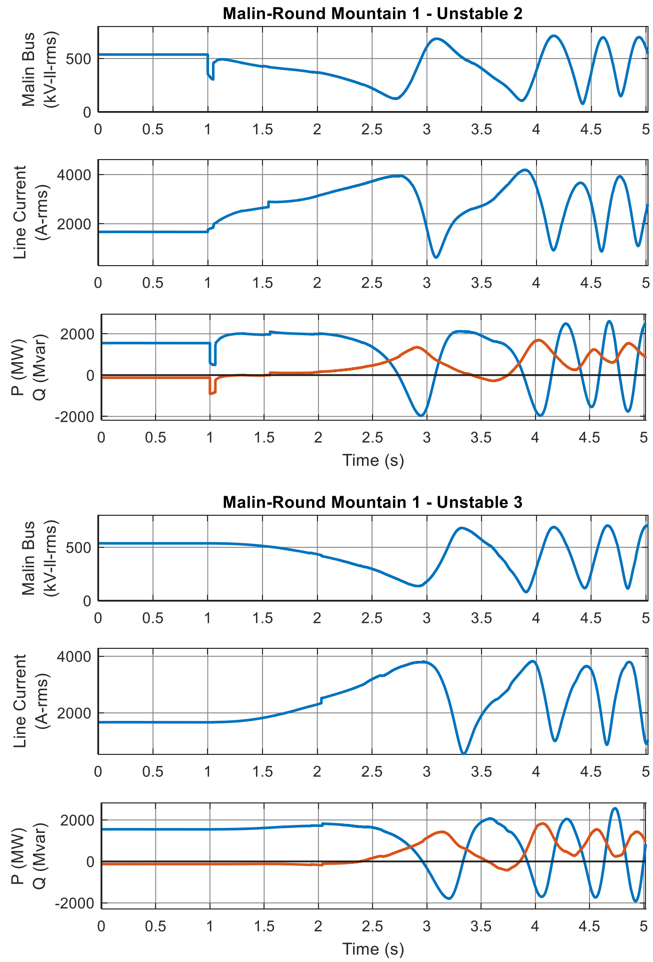

Fig. 14. Three unstable power swing simulations seen from Malin on the Malin-Round Mountain 1 line. For each plot [top] RMS Malin bus voltage, [middle] RMS line current for the Malin-Round Mountain 1, [bottom] three-phase real power (blue) three-phase reactive power (red).

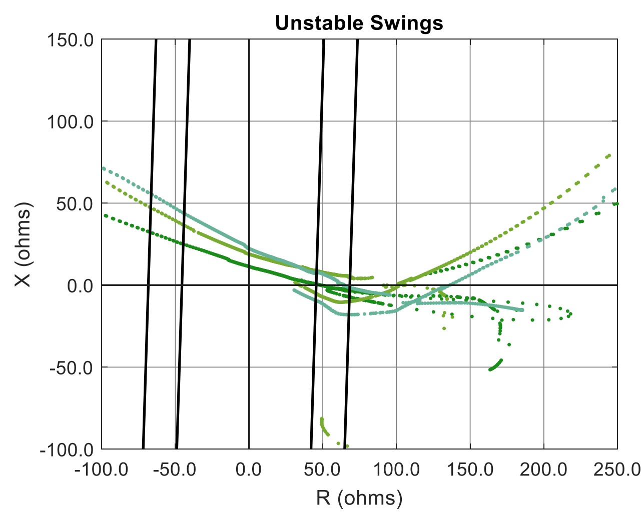

Fig. 15. Plot of the three unstable simulated swings from Fig.14 on an R-X plot seen from the Malin-Round Mountain 1 line. Black is the 2017 OOS characteristic.

The three stable power swing simulations were also converted for relay testing to verify the OOS trip elements do not operate.

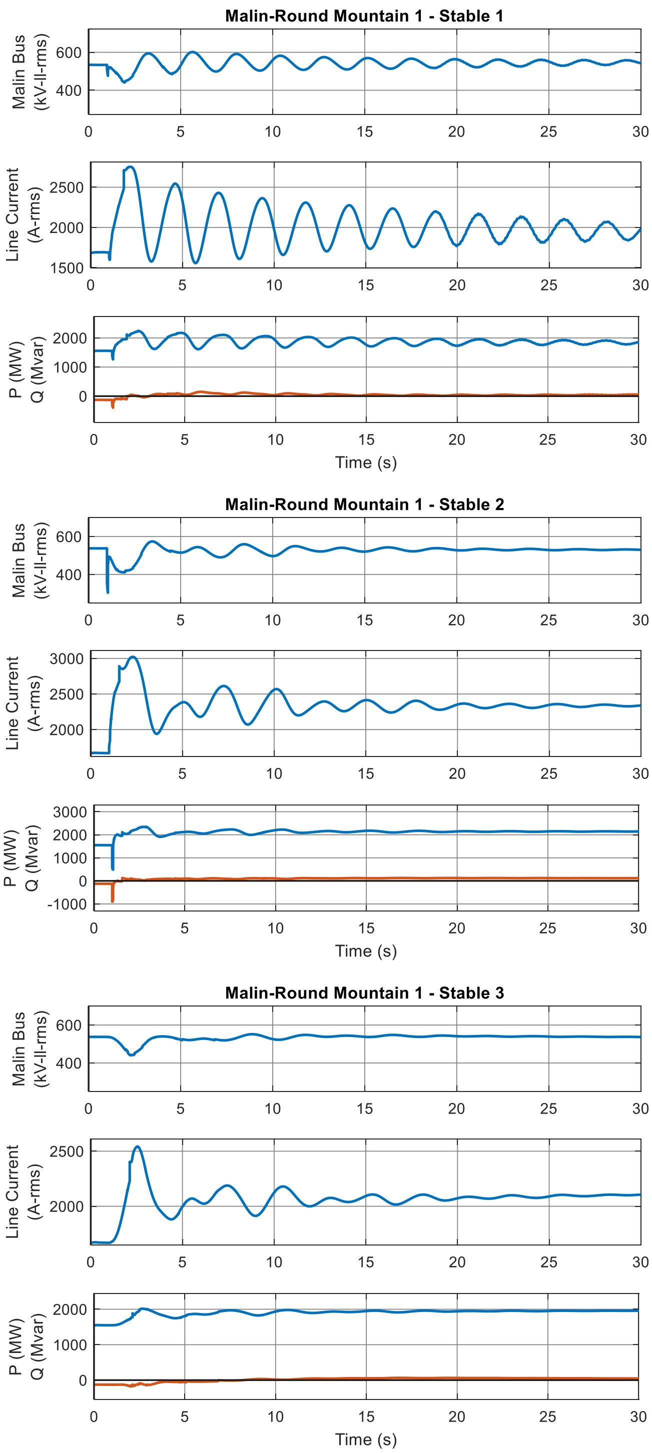

Fig. 16. Three stable power swing simulations seen from Malin on the Malin-Round Mountain 1 line. For each plot [top] RMS Malin bus voltage, [middle] RMS line current for the Malin-Round Mountain 1, [bottom] three-phase real power (blue) three-phase reactive power (red).

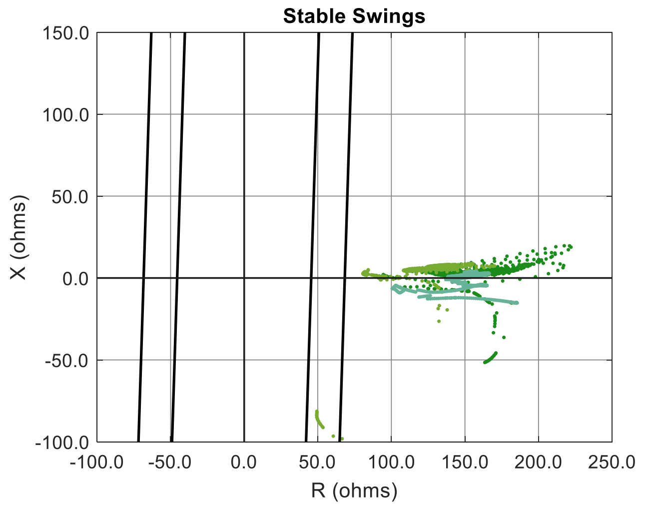

Fig. 17. Plot of the three stable simulated swings from Fig. 16 on an R-X plot seen from the Malin-Round Mountain 1 line. Black is the 2017 OOS characteristic.

B. Converting Transient Stability Simulation Output to Relay Input

A custom script was created to convert the transient stability program CSV results to relay COMTRADE inputs. Fig. 18 illustrates the process used to create the relay input files for each of the six swing cases. Each phase in the process used is briefly explained below. Note that this is just one example of how to perform the conversion. There could be variations and likely necessary modifications that would need to be made to apply the same process to a different system. For example, a necessary modification may be as simple as a different phase notation, or more complicated if the transient stability data provided additional challenges than the ones seen here.

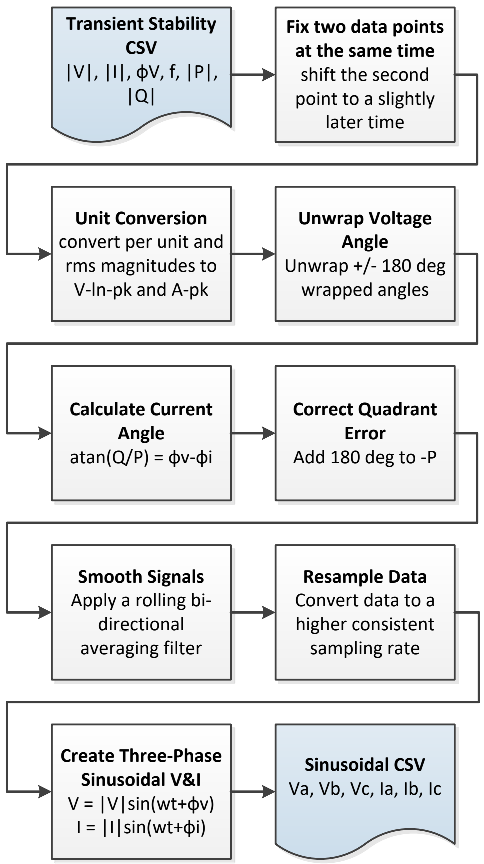

Fig. 18. Flowchart for the custom script created to convert transient stability results into relay inputs. This represents the 'Computational Software' process in Fig. 13.

1) Two Data Points at the Same Time

The simulated swings included step changes where there would be two different data values for the same time stamp, which is unacceptable for a relay input. This was addressed by delaying the second data point. A 1/8 cycle time delay was chosen, as it was less than the time difference between the two closest data points in any of the cases.

2) Unit Conversion

The sinusoidal voltage and current relay inputs need to be in peak values. The per-unit voltages provided from the transient stability program were converted to volts in line-to-neutral peak values, and the RMS current magnitudes were converted to peak.

3) Unwrap Voltage Angle

If the voltage angle provided from the transient stability program is wrapped it can produce erroneous large phase shifts in the sinusoidal waveforms. The phase angles provided by the transient stability program were a wrapped angle between +/- 180 degrees. Some computational software have built in functions to unwrap angles as was used in this case, otherwise a custom script will have to be created.

The top plot in Fig. 19 shows what the +/- 180 wrapped voltage phase angle looked like from the transient stability software. The bottom plot shows the unwrapped angle used to create the sinusoidal voltages and currents.

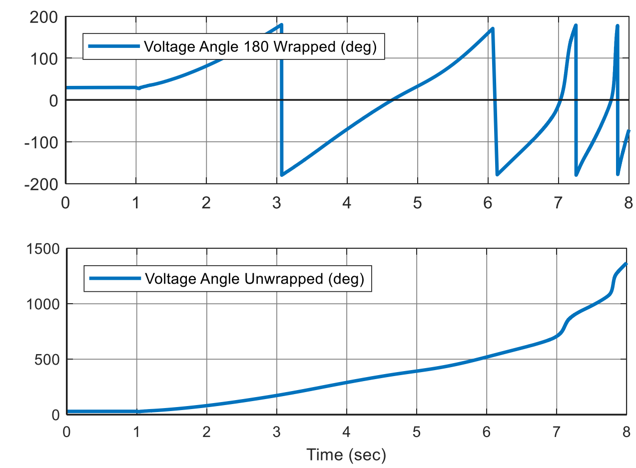

Fig. 19. [top] Wrapped and [bottom] unwrapped voltage phase angles from transient stability software.

4) Calculate Current Angle

The current angle ($\emptyset_i$) can be derived by calculating the V-I angle ($\emptyset_{vi}$) using the given real and reactive power quantities (P and Q), then subtracting from the given voltage angle ($\emptyset_v$) as shown in the Eq. 1-3 below.

$$\text{atan}\left(\frac{Q}{P}\right) = \emptyset_{vi} \quad [Eq. 1]$$

$$\emptyset_{vi} = \emptyset_v - \emptyset_i \quad [\text{Eq. 2}]$$

$$\emptyset_i = \emptyset_v - \text{atan}\left(\frac{Q}{P}\right) \quad [Eq. 3]$$

5) Correct Quadrant Error

Most calculators will provide angles of trigonometric functions only in the first and fourth quadrants, because they do not discriminate between the polarity of the numerator and denominator independently. Without correction, the impedance derived from the sinusoidal voltage and currents by the relay can be in the incorrect quadrant.

It was discovered that when real power flow was negative the V-I phase angle simply needed to be shifted by 180 degrees as shown in Fig. 20.

The top plot of Fig. 20 shows an example of what the V-I angles look like out of the arctan function without correction. The middle plot shows the corrected power angle. The bottom plot shows the real power. When the real power is negative the corrected angle is the arctan angle plus 180 degrees. Negative real power using BPA notation represents power flow into the bus. The appendix of this document goes through an example of this quadrant error and correction.

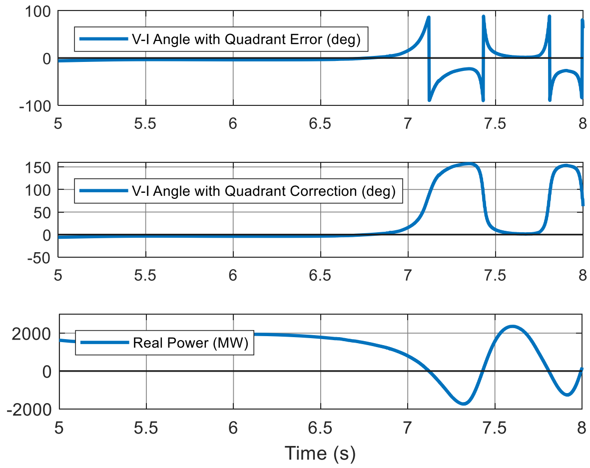

Fig. 20. The [top] V-I angle with quadrant error and [middle] shows V-I angle with quadrant correction that is shifted by 180 degrees when [bottom] real power is negative.

6) Smooth Signals

A custom rolling bi-directional averaging window filter was applied to each swing case to smooth out some of the inconsistencies. Bi-directionality compensates for the natural time shift that will occur when applying an averaging filter forwards in time, by applying the same filter backwards in time.

7) Resample Data

The sampling rate for the cases provided by the transient stability software were variable. More points were concentrated on areas where there were more changes in the data values and less when there minor were minor changes in data. COMTRADEs for relay input require a consistent sampling rate. To accomplish a consistent sample rate the data was up sampled to a higher rate, repeating data values where there were no changes. It is important to save increasing the number of data samples to the last step possible to reduce processing time. A sampling rate of 2-10 kHz would be sufficient for most modern relays.

8) Create Three-Phase Sinusoidal Voltage & Current

Using the magnitude and phase for both voltage and current, a sinusoidal waveform can be produced. The voltage and current equations provided below use A-B-C clockwise notation (Eq. 4-9).

$$V_A(t) = |V|\sin(\omega t + \emptyset_V) \quad [Eq. 4-6]$$
$$V_B(t) = |V|\sin(\omega t + \emptyset_V - 120°)$$
$$V_C(t) = |V|\sin(\omega t + \emptyset_V + 120°)$$

$$I_A(t) = |I|\sin(\omega t + \emptyset_I) \quad [Eq. 7-9]$$
$$I_B(t) = |I|\sin(\omega t + \emptyset_I - 120°)$$
$$I_C(t) = |I|\sin(\omega t + \emptyset_I + 120°)$$

9) Convert CSV to COMTRADE

Using freeware ATP Analyzer event viewing software the CSV output from the custom script was converted to a COMTRADE format. ATP Analyzer can also use the sinusoidal currents and voltages to calculate transient real power, reactive power, resistance, and reactance quantities.

10) Check Results

It is highly recommended to check the conversion results before proceeding to relay testing. One check is to calculate real and reactive power from the three-phase sinusoidal voltage and currents. Compare the calculated values to the originally provided values to verify results.

C. OOS Trip Relay Testing

Relay testing included:

1. Six total simulated stable and unstable swing cases
2. A measured stable swing from 2004
3. A measured unstable swing from 1996
4. 75 simulated internal and external faults

1) Simulated Power Swing Relay Testing

After the six transient stability simulated power swings were converted into COMTRADEs they were played directly into the relays. The relay event records from the three unstable power swings are shown in Fig. 21-23.The relay did not produce events for the stable swings, because there correctly was no trip and therefore no event trigger. The trip times for the unstable power swings, and the no operation for the stable power swings was determined to be satisfactory.

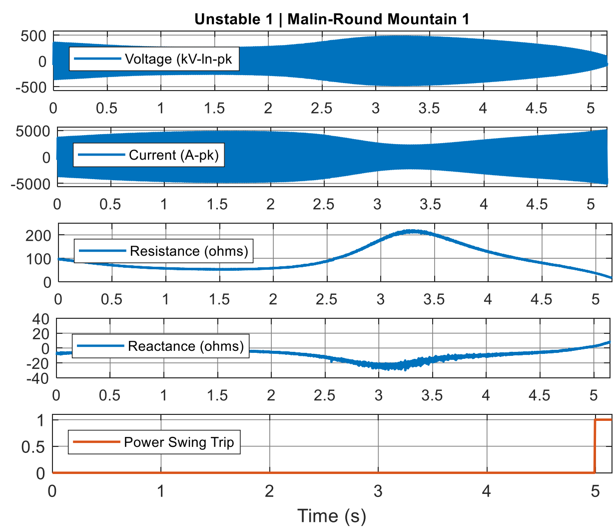

Fig. 21. Power swing trip signal comes in 4.99 seconds into the event record.

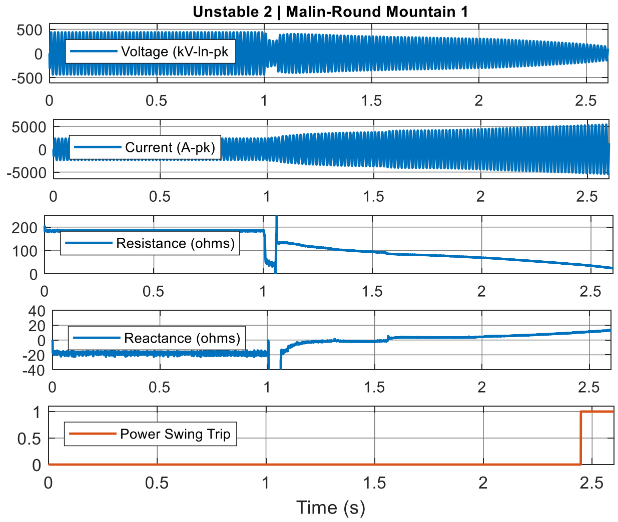

Fig. 22. Power swing trip comes in 2.45 seconds into the relay event record.

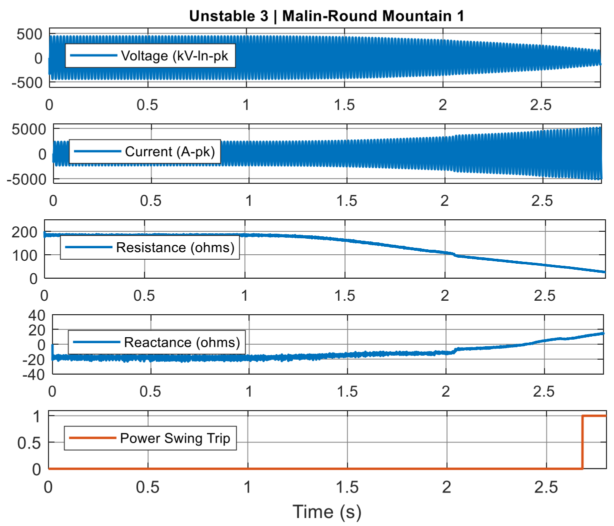

Fig. 23. Power swing trip comes in 2.68 seconds into the relay event record.

2) June 2004 Loss of Large Generation Stable Swing

Using Phasor Measurement Unit (PMU) data from a real system event that nearly resulted in a system outage in 2004 was converted to a COMTRADE for relay testing. The stable power swing at the COI was created by a long duration fault in Arizona followed by a loss of a large amount on generation in southern California.

When this real event was tested in the relays there correctly was no trip operation, and no event record generated. The RMS PMU values for the swing are shown in Fig. 24.

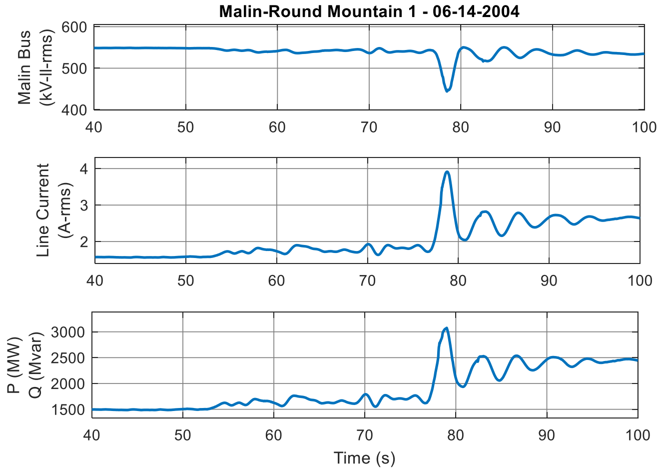

Fig. 24. Stable swing seen from Malin on the Malin-Round Mountain 1 line from 06/14/2004.

The impedance plot is shown in Fig.25 where the swing enters the outer blinder of the 2018 OOS trip characteristic (shown in black), but does not pass through the inner blinder. The swing does not enter the 1992 OOS trip characteristic (shown in red), which were the in-service settings at the time of the event.

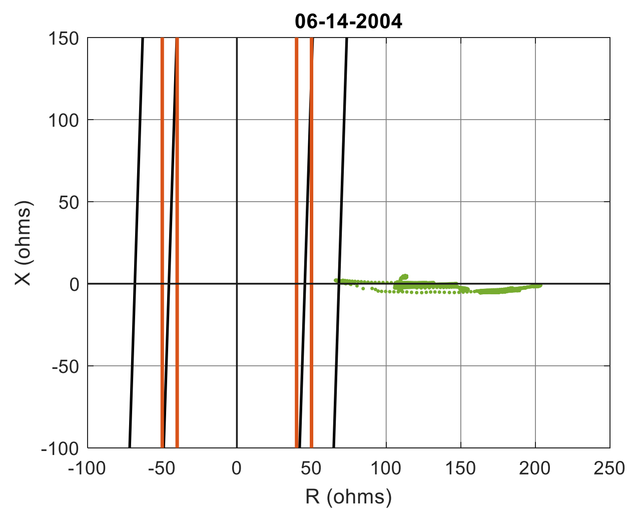

Fig. 25. 30 samples/sec PMU data for 2004 stable power swing. [green] (R,X) points for Malin-Round Mountain 1, [red] 1992 OOS characteristic [black] 2017 OOS characteristic.

3) August 1996 Unstable Swing

PMU data captured from the 08-10-1996 blackout was also converted into a COMTRADE for OOS relay testing on the Malin-Round Mountain 1 line. The power swing was an unstable case, but the intertie separated early due to a non-OOS relay Misoperation. Unfortunately, because the event record was cut too short the OOS relay testing did not result in a trip operation. The PMU measurement values are shown in Fig. 26 and the calculated impedance R-X plot is shown in Fig. 27.

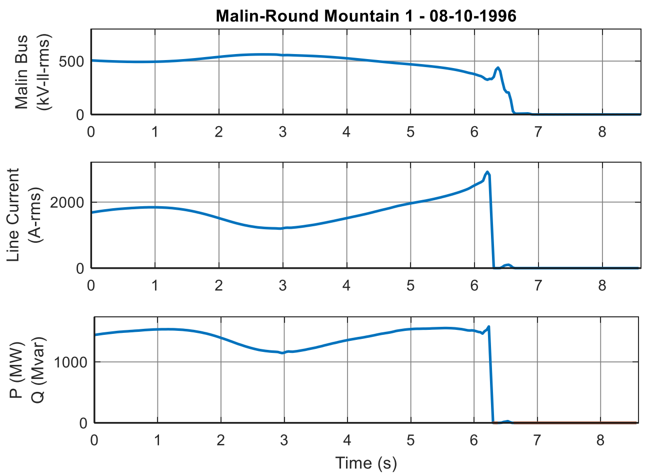

Fig. 26. Unstable swing seen from Malin on the Malin-Round Mountain 1 line from August of 1996.

The 1996 swing enters the outer blinder of the 2017 settings (black characteristic in Fig. 27), but does not pass through the inner blinder. The swing does not appear to enter the blinders for the 1992 OOS settings (red characteristic in Fig. 27), which were the in-service settings at the time the swing occurred.

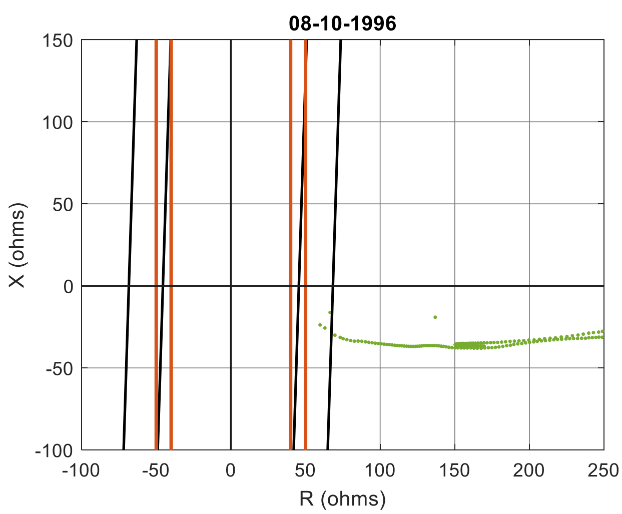

Fig. 27. 30 samples/sec PMU data for 1996 power swing [green] (R,X) points for Malin-Round Mountain 1, [red] 1992 OOS characteristic [black] 2017 OOS characteristic.

4) Simulated Internal and External Faults

The 75 simulated internal and external faults were ran with equipment in loop to verify there would be no OOS trip operation for multiple types of internal and external faults. The faults were simulated using a Real Time Digital Simulator. The faults were ran in multiple locations with various equipment and transmission paths out of service and with low load, normal load, and high load conditions.

VI. Misoperations

In November of 2018, the Captain Jack-Olinda OOS relays were integrated into the modern line relays that had been installed in 2012 with settings updated based on the new swing studies developed in 2017. The Malin-Round Mountain 1 & 2 lines were not updated due to scheduling delays.

In January 2019 there were two OOS misoperations where the Captain Jack-Olinda line tripped under light load conditions. The misoperations illuminated the importance of the reactive reach of the OOS quad elements, and the minimum pickup current.

The Malin-Round Mountain lines still used the original 1992 relays and settings. In hindsight, we were lucky that the original relays were on two out of three of the COI lines.

On Sunday January 20th, 2019 real power flow on the Captain Jack-Olinda line was decreasing. The power flow turned to mostly reactive, so the resistive or real power component was decreasing considerably. The power flow reached into the OOS trip blinders and tripped the Captain Jack-Olinda line. The same incident occurred for a second time on Monday January 21st, 2019, which was a holiday. On Tuesday January 22nd the OOS element was disabled on the Captain Jack-Olinda line. The Malin-Round Mountain 1 & 2 lines were left enabled since there was no history of misoperations using the older relays and settings.

Below are two figures, Fig. 28 and 29, of 60 samples-per-second PMU data for the two misoperation events. Post analysis of the misoperations do not actually show power flow clearly going through the blinders. Not even when the relay event record was played back through the relay in the lab did it operate. One hypothesis is that the sampling rate of the event did not capture exactly what the relay measured.

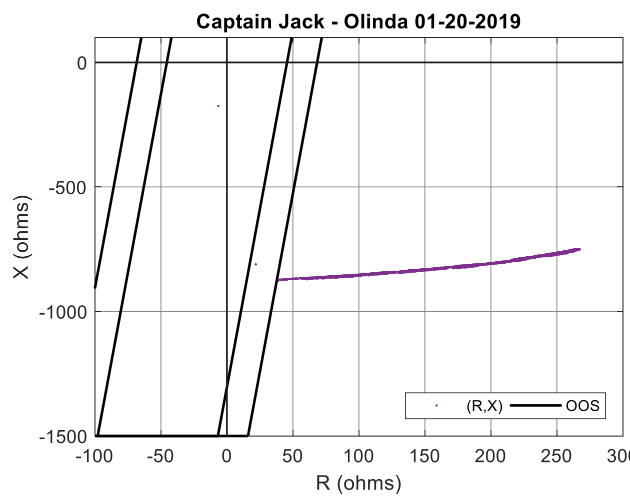

Fig. 28. 60 samples/sec PMU 01/20/2019 (R,X) points for [purple] Captain Jack-Olinda, [black] 2017 OOS characteristic.

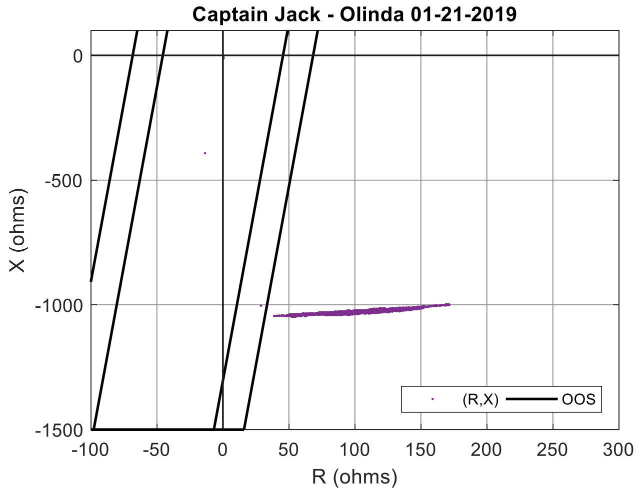

Fig. 29. 60 samples/sec synchrophasor 01/21/2019 (R, X) points for [purple] Captain Jack-Olinda, [black] 2017 OOS characteristic.

A. Analysis of Historical Power Flow

Post misoperation review of historical 5-minute SCADA data from 2015 to 2018 (Fig. 30-33) showed that this misoperation was going to happen at some point with the updated OOS settings. Most power flow on the Captain Jack-Olinda line is below the surge impedance loading of the line and is therefore capacitive or having a negative reactance component. The power flow trend from 2015-2018 shows an increase in importing power from the south, and more overall variability in the characteristics. The change in power flow over time generally speaking is a slow power swing and is at risk of causing an OOS trip misoperation.

In Fig. 30-33 the apparent impedance is plotted for each of the three lines for that entire calendar year. The purple (R,X) impedance dots are for the Captain Jack-Olinda line. The green and blue (R,X) impedance dots are for the Malin-Round Mountain 1 & 2 lines, respectively. Each figure also has the OOS trip characteristic(s) that were applicable for that year.

In 2015 power flow on all of the COI lines showed primarily exporting power to the south (Fig. 30) with positive resistance. Over the next few years that trend starts to change as there is an increase in importing power from the south shown as negative resistance. Until 2018, where there is a significant increase in importing power from the south.

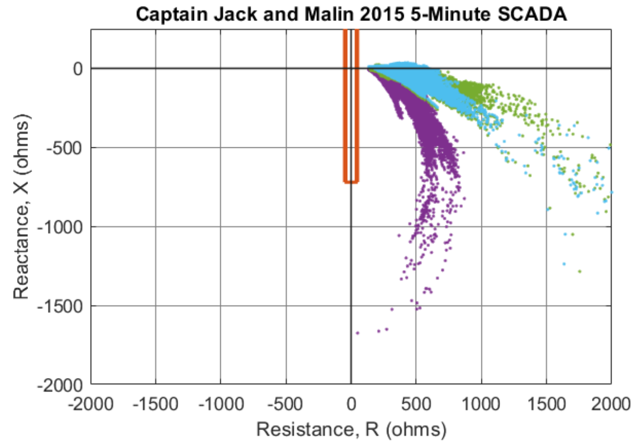

Fig. 30. 2015 5-minute SCADA (R,X) points for [purple] Captain Jack-Olinda, [green/blue] Malin-Round Mountain 1 & 2, [red] 1992 OOS characteristic.

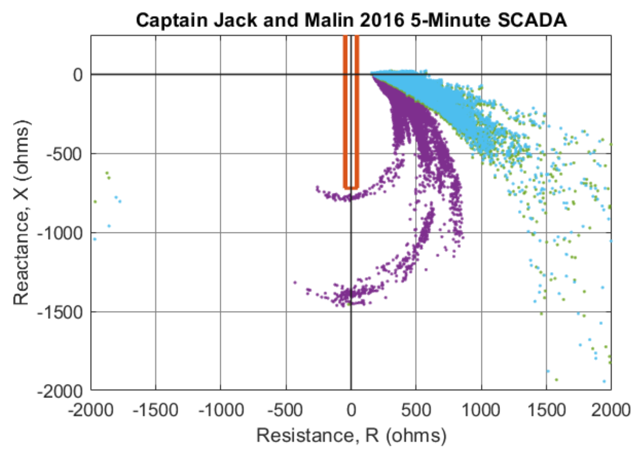

Fig. 31. 2016 5-minute SCADA (R,X) points for [purple] Captain Jack-Olinda, [green/blue] Malin-Round Mountain 1 & 2, [red] 1992 OOS characteristic.

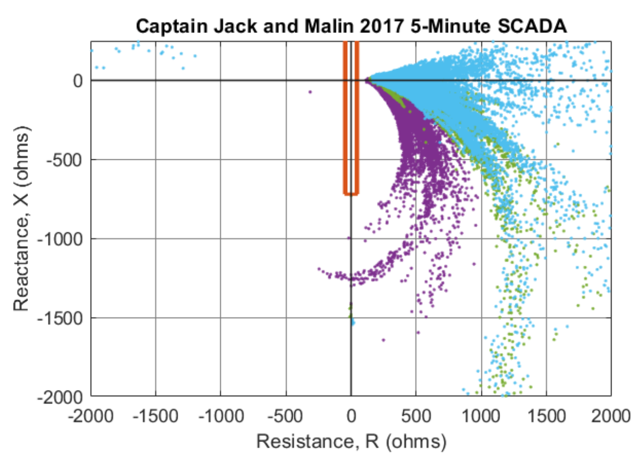

Fig. 32. 2017 5-minute SCADA (R,X) points for [purple] Captain Jack-Olinda, [green/blue] Malin-Round Mountain 1 & 2, [red] 1992 OOS characteristic.

In 2018 the settings for the Captain Jack-Olinda line were changed to the black characteristic shown in Fig. 33. The

Malin-Round Mountain lines continues to use the shorter red characteristic. As shown in the figure impedance data from the Captain Jack-Olinda line shown as purple dots pass into the black OOS trip characteristic.

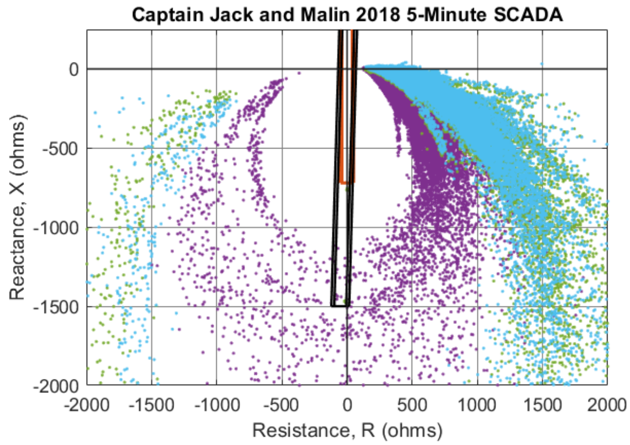

Fig. 33. 2018 5-minute SCADA (R,X) points for [purple] Captain Jack-Olinda, [green/blue] Malin-Round Mountain 1 & 2, [red] 1992 OOS characteristic, and [black] 2017 OOS characteristic that was installed on the Captain Jack-Olinda line in 2018 and caused a misoperation in 2019.

VII. Post Misoperation Updated Out-of-Step Settings

According to the simulated swing files, unstable swings occur under high power flows above the line's surge impedance loading where line current is inductive and therefore a positive reactance. According to historical data power flow on these lines are typically capacitive or a negative reactance. The solution is then to significantly reduce the reach of the OOS trip element in the negative reactance or capacitive direction. Consistent with reducing the negative reactive reach, the supervisory minimum pickup current was also raised to ensure there would be no operation under light load conditions. A plot of the post misoperation updated settings are shown below in Fig. 34.

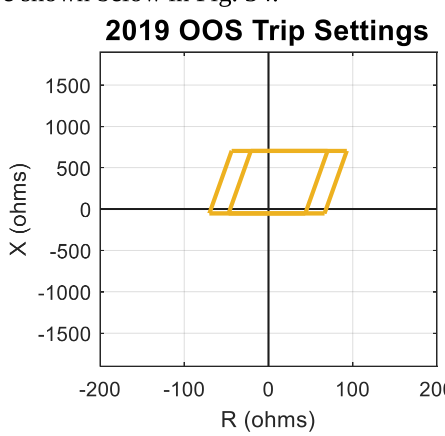

Additional OOS Trip Settings	
Minimum PU Current (A)	900
Maximum Resistive Rate of Change (ohm/sec)	200

Fig. 34. Post misoperation 2019 OOS trip characteristic and additional settings.

In November, 2019 the post misoperation updated settings were applied in the OOS relay at Captain Jack. Fig.35 shows the entire calendar year of 2019 historical power flow with the 2017 settings that were applied in 2018 in black, and the post misoperation 2019 updated settings in dark blue. The second figure, Fig. 36, shows the effect of apply a minimum pickup current of 900 amps. Note that all of the simulated swing cases had currents above 1500 amps. The minimum pickup current previously used on the Captain Jack-Olinda line developed in 2017 was 300 amps, and the 1992 OOS trip relays used 600 amps.

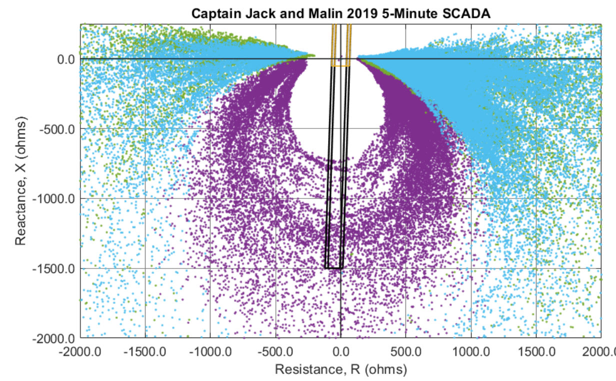

Fig. 35. 5-minute SCADA (R,X) points for [purple] Captain Jack-Olinda, [green/light blue] Malin-Round Mountain 1 & 2, [black] 2018 OOS characteristic, [yellow] 2019 updated OOS characteristic.

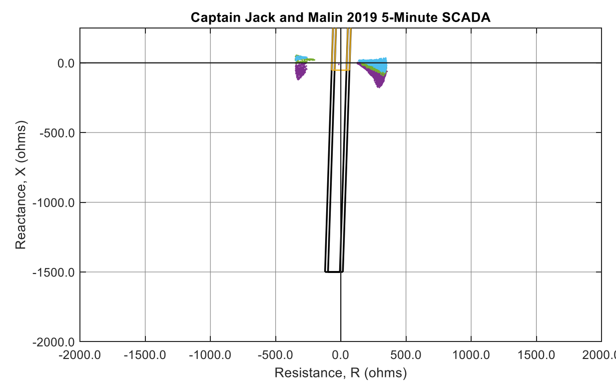

Fig. 36. 2019 5-minute SCADA data in previous figure with the effect of a applying a minimum pickup current of 900 amps.

VIII. Conclusions

It had been 25 years since the last update to the OOS relays on the COI, and almost all of the internal expertise was gone. Clues to how the relays were previously tested and intended to work were passed down from the few remaining people that were involved in the project and luckily kept good records. This paper outlines the process used to update the settings this time around as a way to document and disseminate this experience with others. For that purpose, a summary of recommendations based on the lessons learned are outlined below.

- When possible verify OOS relay setting performance through lab testing by running location specific stable and unstable power swing simulations in the relays.
- Verify other protection elements are not compromised by the OOS tripping elements by running comprehensive fault simulations.

- On series compensated lines verify the voltage source that is used in the swing studies match what will be used in the OOS relay.
- When possible verify OOS relay setting performance against real field measured swing data.
- Analyze how historical power flow will react with OOS tripping elements to prevent a separation under normal and expected load conditions.

IX. Appendix – Quadrant Error Correction

The quadrant error from using an arctan function to solve for the voltage-current angle is illustrated using the example data in Table 1, and plot in Fig. 37 below. A good sanity check is that when reactive power (Q) is negative or capacitive, the current should be leading the voltage, and when Q is positive or inductive the current should be lagging the voltage.

Table 1 Example PQ values with arctan function angle outputs and corrected angles in degrees. When real power flow is negative 180 degrees is added to the arctan output to get the corrected angle.

Quad	**P** (MW)	**Q** (Mvar)	$\emptyset_{vi}$ arctan(Q/P) (deg)	$\emptyset_{vi}$ corrected (deg)	$\emptyset_i$ * (deg)
I	+1000	+200	+11	+11	-11
II	-1000	+200	-11	-11+180 = 169	-169
III	-1000	-200	+11	+11+180 =191	-191
IV	+1000	-200	-11	-11	11

*Current angles are given with respect to a voltage reference angle of zero.

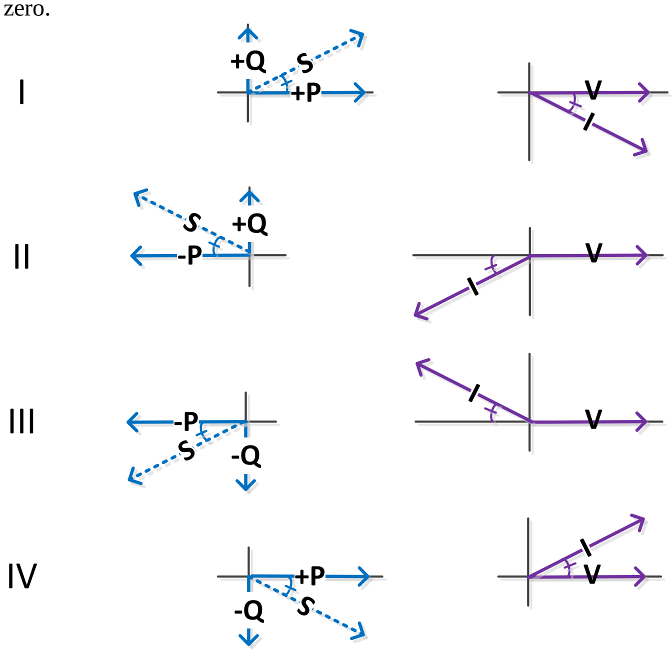

Fig. 37. P, Q and S vectors for all four quadrants are shown on the left-hand side of the figure and their respective V and I vectors for a voltage reference angle of zero degrees are shown on the right-hand side of the figure. Vector magnitudes and angles are for visualization purposes only and are not to scale.

X. Acknowledgment

The authors would like to gratefully acknowledge the contributions of those people without whom it would not have been possible to complete this work. They are Sam Hirsi, Dmitry Kosterev, Tom Roseburg, Dan Goldsworthy, Warren Reese, and Steve Laslo.

XI. References

[1] C.W. Taylor J.M. Haner L.A. Hill W.A. Mittelstadt R.L. Cresap, “A new Out-of-Step Relay with Rate of Change of Apparent Resistance Augmentation,” in *IEEE Transactions on Power Apparatus and Systems*, vol. PAS-102, No. 3. Mar. 1983.

[2] J.M. Haner T.D. Laughlin C.W. Taylor, “Experience with the R-RDOT Out-of-Step Relay,” in *IEEE Transactions on Power Systems*, vol. PWRD-1, No. 1. Apr. 1986.

[3] D. Erwin M. Anderson R. Pineda D. Tziouvaras R. Turner, “PG&E 500kV Series-Compensated Transmission Line Relay Replacement: Design Requirements and RTDS Testing”

XII. Biographies

Caitlin Martin, P.E. Graduated from Portland State University with a Bachelor’s degree in Electrical Engineering in 2008, and graduated from University of Idaho with a Master’s degree in Electrical Engineering in 2013. She has worked at Bonneville Power Administration since 2006 focusing on protective relaying, EMTP studies, and transient analysis. Caitlin is a licensed Profession Engineer in the state of Washington.

Aaron Martin, P.E. received his Bachelor’s degree from the University of Idaho in Electrical Engineering and in 2007 he received his Masters of Engineering also from the University of Idaho. He has worked for the Bonneville Power Administration in substation automation and system protection and control since 2002. From 1999 to 2002 he worked for the U.S. Army Corp of Engineers as a Maintenance Engineer at Lower Granite Dam in Washington State. Aaron is a licensed Profession Engineer in the state of Washington and a member of the IEEE PSRCC.